ELSEVIER

Materials Characterization 58 (2007) 694 – 700

MATERIALS CHARACTERIZATION

Synthesis of gold nanoparticles with different atomistic structural characteristics

R. Esparza [a,*], G. Rosas [a], M. López Fuentes [b], J.F. Sánchez Ramírez [c], U. Pal [b], J.A. Ascencio [d], R. Pérez [d]

[a] *Instituto de Investigaciones Metalúrgicas, UMSNH, Edificio U, Ciudad Universitaria, Morelia, Mich., 58000, Mexico*
[b] *Instituto de Física, Universidad Autónoma de Puebla, Apdo. Postal J-48, Puebla, Pue., 72570, Mexico*
[c] *CICATA-IPN, Legaría 694, Col. Irrigación, México D.F., 11500, Mexico*
[d] *Instituto Mexicano del Petróleo, Eje Central Lázaro Cárdenas No 152, Col. San Bartolo Atepehuacan, México D. F., 07730, Mexico*

Received 12 June 2006; received in revised form 6 October 2006; accepted 28 November 2006

Abstract

A chemical reduction method was used to produce nanometric gold particles. Depending on the concentration of the main reactant compound different nanometric sizes and consequently different atomic structural configurations of the particles are obtained. Insights on the structural nature of the gold nanoparticles are obtained through a comparison between digitally-processed experimental high-resolution electron microscopy images and theoretically-simulated images obtained with a multislice approach of the dynamical theory of electron diffraction. Quantum molecular mechanical calculations, based on density functional theory, are carried out to explain the relationships between the stability of the gold nanoparticles, the atomic structural configurations and the size of nanoparticles.

Keywords: Nanoparticles; Gold; Structural determination; High-resolution electron microscopy; Density functional theory; Molecular simulation

1. Introduction

Nanoparticles are defined as atomic arrangements with nanometric dimensions and usually with a small number of constituent atoms. The structural configurations of these small particles induce new types of physical properties. Therefore, the selection of a synthesis method which can give rise to a particular structural particle configuration is very important for new technological applications [1,2]. Depending on the nanometric particle size, the nanostructures can have different applications. These applications include fields such as: catalysts, photography, medicine, information storage in magnetic devices etc. In recent years, the high-resolution electron microscope (HREM) has been one of the main tools used to study the physical properties of nanometric particles. Metallic nanoparticles usually display simple geometric atomic arrangements, mainly with tetrahedral, octahedral and decahedral forms [3,4]. They even present atomic configurations which display five-fold symmetry [5]. In the reduction synthesis method used in this investigation, particles of different average sizes and different geometrical arrangements have been obtained.

* Corresponding author. Tel.: +52 443 322 3500x4032; fax: +52 443 322 3500x4010.
E-mail address: roesparza@gmail.com (R. Esparza).

1044-5803/$ - see front matter © 2006 Elsevier Inc. All rights reserved.
doi:10.1016/j.matchar.2006.11.032

The morphological nature of the nanometric particles depends on the concentration of the main reagent compound used in the reduction process. In this study, the structural characterizations of gold nanoparticles with different structural morphologies have been carried out through a comparison between experimental and theoretical HREM images. The stability of the nanoparticles is also evaluated using density functional theory based on quantum mechanical calculations.

2. Experimental procedures

Ultra fine gold particles have been obtained using the chemical reduction method reported earlier [6,7]. Methanol solutions of gold ions were prepared by dissolving crystalline hydrogen tetrachloroaurate ($HAuCl_4 \cdot xH_2O$) in methanol (0.033, 0.044, 0.099, 0.11 and 0.12 mmol in 25 ml of methanol). A methanol solution of PVP [poly (*N*-vinyl-2-pyrrolidone) (150 mg of PVP in 25 ml of methanol), was added to the metal ion mixture. To reduce the metal ions, 6 ml of an aqueous solution of $NaBH_4$ (0.066 M) was added to the mixture solution dropwise at room temperature. A homogeneous colloidal dispersion was formed after the addition of the $NaBH_4$ reductant in the solution containing the metal ions.

The structural and morphological characteristics of the dispersed metallic nanoparticles have been studied using a transmission electron microscope, Philips Tecnai F20, which has a field emission gun attachment, an operating voltage of 200 keV, a spherical aberration of 1 mm, and a direct maximum resolution dot to dot of 0.23 nm. TEM specimens were obtained from the homogeneous colloidal solution. Drops of this solution were deposited on a copper grid (3 mm in diameter) with an amorphous carbon film. The HREM images have been digitally processed. Theoretical simulations based on the multislice approach of the dynamical theory of electron diffraction [8] have been carried out to generate HREM images of gold nanoparticles.

Studies on the stability of the nanoparticles were carried out using quantum molecular calculations. These simulations were carried out using the Dmol^3 software by Accelrys [9], which is based on the density functional

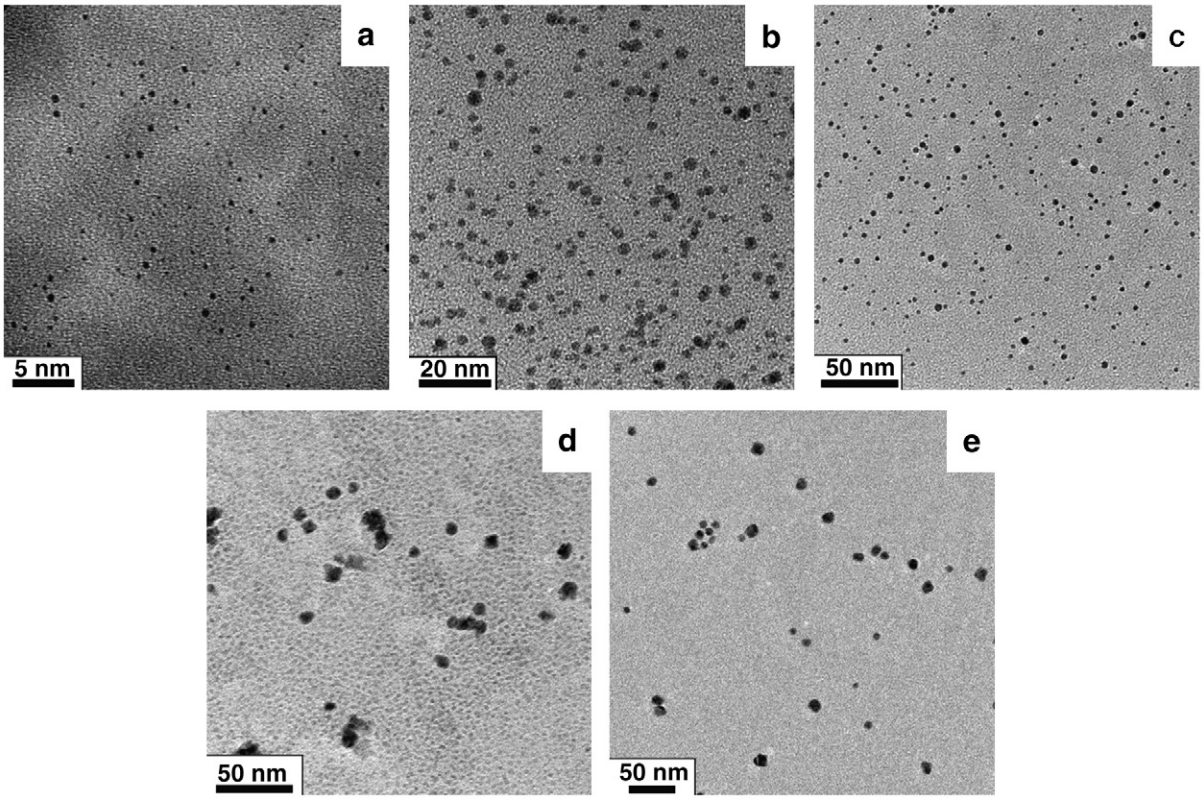

Fig. 1. Low magnification TEM images of the gold nanoparticles synthesized with different concentrations of gold ions; a) 0.033 mmol, b) 0.044 mmol, c) 0.099 mmol, d) 0.11 mmol and e) 0.12 mmol in 50 ml of reaction mixture.

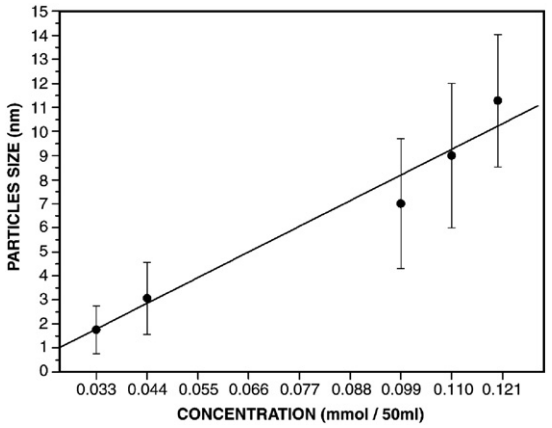

Fig. 2. Variation of average particle size as a function of gold ion concentration in the reaction mixture.

theory (DFT). In our case we used the generalized gradient approximation (GGA) with the Perdew–Wang (PW91) function [10] and a field consistent tolerance of 1×10^{-6} eV. The configurations of 13, 19 and 38 atoms for cubo-octahedral and 13, 19 and 39 atoms for decahedral structures were studied; the selection of these clusters is focused because of the experimental results and previous reports that demonstrate these are the most commonly produced [11–13], even though from many reports suggest other more stable configurations [14–16]. The minimum energy for each of the structures was obtained by means of a geometry optimization task based on the DFT method. The geometry optimization was followed by a single point energy calculation to obtain the electrostatic potential, highest occupied molecular orbital (HOMO) and lowest unoccupied molecular orbital (LUMO), and Fukui functions.

3. Results and discussion

Fig. 1 shows low magnification electron microscope images of the nanometric gold particles obtained with different concentrations of the Au ions. These low magnification images just show the relative particle size increments as the concentration of gold ions in the reaction mixture is increased. The average particle size varied from a few nanometers at 0.033 mmol (in 50 ml of reaction mixture) to approximately 12 nm for the 0.12 mmol metal ion content. This is further illustrated in Fig. 2, where the average particle size values are displayed as a function of Au ion content in the solution. The nature of the atomistic structural configuration is also strongly dependent on the total ion content in the reaction mixture.

For example, for a metal ion content of 0.044 mmol, Fig. 3 shows some commonly found configurations. Fig. 3a illustrates a single twinned particle (stp) and Fig. 3b and c shows fcc-like particles. On the other hand, for a metal ion content of 0.11 mmol, Fig. 4 shows two fcc-like particles and one multi-twinned particle. A statistical summary of these structural characteristics is given in Fig. 5. At low concentrations of the metal ions

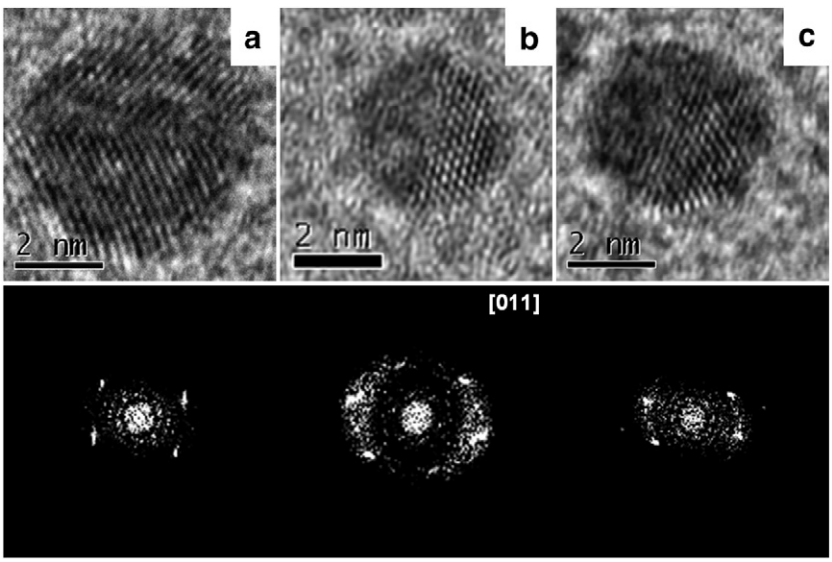

Fig. 3. HREM images of gold nanoparticles with their respective power spectra, prepared from a solution with 0.044 mmol/50 ml gold ion concentration; a) single twinned particle, b) and c) fcc-like particles.

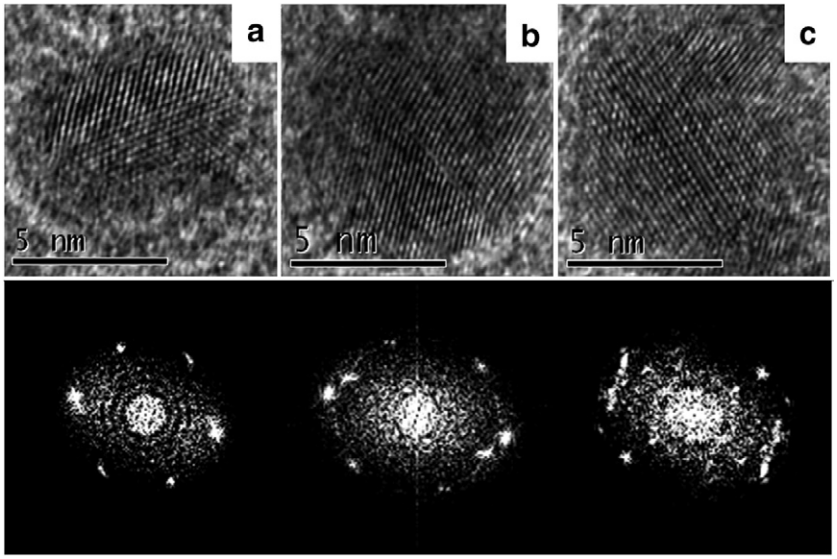

Fig. 4. HREM images of gold nanoparticles with their corresponding power spectra, prepared from a solution with 0.11 mmol/50 ml gold ion concentration; a) and b) fcc-like particles, c) multi-twinned particle.

(0.033 mmol/50 ml), the more commonly found structures are decahedral and fcc-deformed; however, as the concentration is increased (0.044, 0.099 and 0.11 mmol/50 ml), the most commonly found structures change to single twinned particles and fcc-like particles. It is also important to mention that the size of the particles obtained for the lowest concentration of metal ions is smallest; only a few nanometers in diameter with less than 2 nm on average. Depending on the metal ion concentration in the reaction mixture, two main regions of nanoparticle growth with distinct characteristics in atomic ordering and hence of distinct structural features

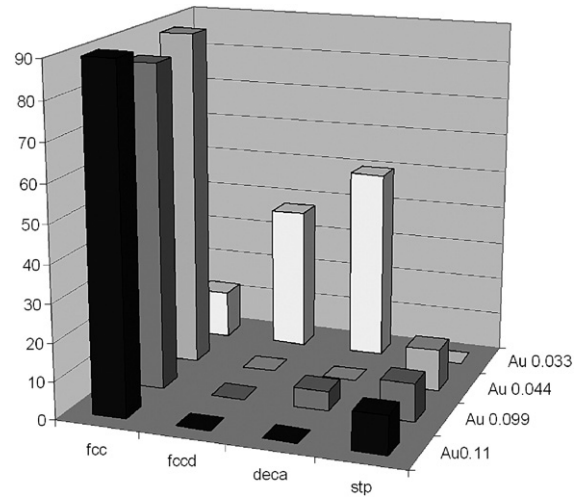

Fig. 5. Statistical distribution of gold nanoparticles with different atomistic structural forms for different gold ion concentrations in the reaction mixture. These experimental results were obtained from the analysis of HREM images; fcc-like (fcc), fcc-deformed (fccd), decahedral (deca) and single twin particle (stp). The ion concentrations are expressed in mmol/50 ml.

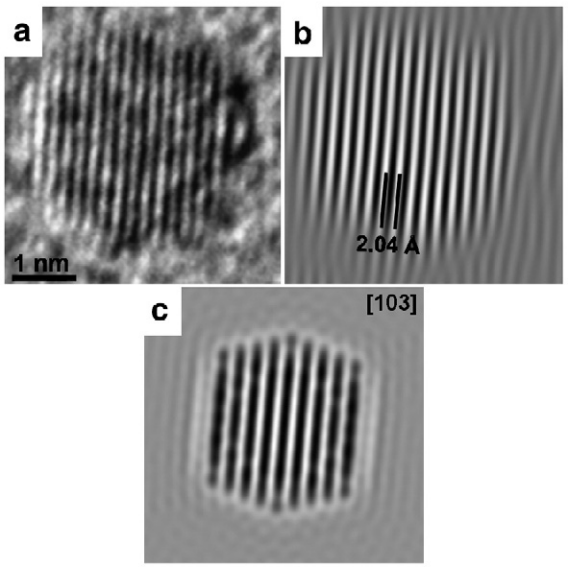

Fig. 6. a) HREM image of a cubo-octahedron gold particle obtained from the reaction solution of lowest gold ion concentration (0.033 mmol/50 ml), b) same HREM image after digital processing, and c) theoretically-simulated image of a cubo-octahedron along the [103] crystalline orientation.

are found. Low concentrations (0.033 mmol/50 ml) induced the formation of decahedral and fcc-deformed gold particles. However, higher concentrations (0.044, 0.099 and 0.11 mmol/50 ml) induced the formation of single twinned particles and fcc-like particles.

A qualitative insight of the atomistic structural characteristics of the nanometric gold particles is obtained by comparing the experimental high-resolution images and theoretically-simulated images. Fig. 6a shows the HREM image of a nanometric gold particle produced under a low concentration condition of gold ions. Fig. 6b illustrates the same HREM image digitally processed. Fig. 6c shows the theoretically-simulated HREM image of a cubo-octahedron along the [103] crystalline orientation. A comparison between the experimental and simulated images suggests the possible nature of the atomistic structural configuration of the image shown in Fig. 6a. Therefore, Fig. 6a resembles the HREM image contrast produced by a cubo-octahedron. Fig. 7a shows the HREM image of a typical gold nanoparticle obtained for a gold ion concentration of 0.044 mmol/50 ml and Fig. 7b displays the same image after it has been digitally processed. Fig. 7c shows the theoretical HREM simulation of an fcc-like particle oriented along the [011] crystalline axis. A comparison between the experimental image and the theoretical image suggests that the particle has a structure resembling fcc. Fig. 8 shows a single twinned gold

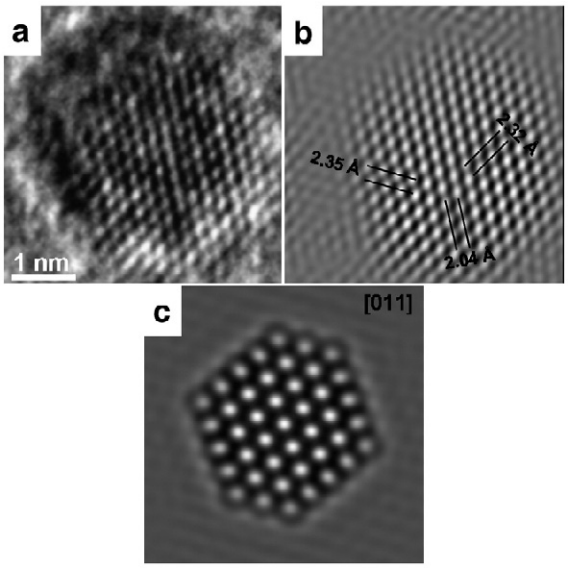

Fig. 7. a) HREM image of a gold nanoparticle obtained from a reaction mixture containing 0.044 mmol/50 ml gold ion concentration, b) same HREM image after digital processing, and c) theoretical simulation of a fcc-like particle oriented along the [011] crystalline axis.

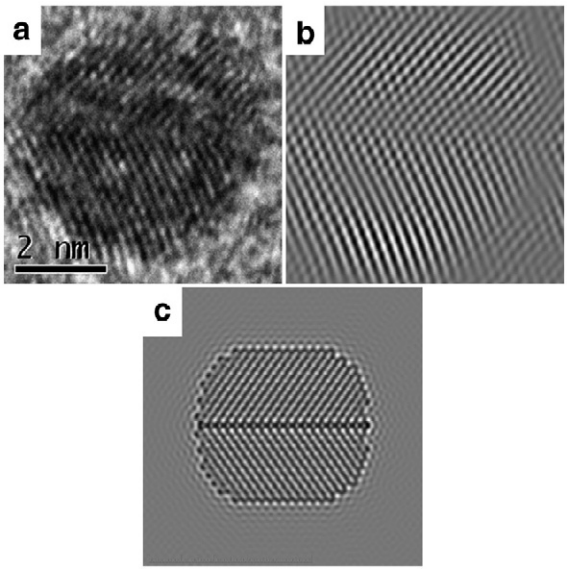

Fig. 8. a) HREM image of a single twinned nanoparticle obtained from the reaction mixture containing 0.044 mmol/50 ml gold ion concentration, b) digitally-processed HREM image, and c) the theoretical simulation was obtained assuming two fcc gold crystals along the [011] orientation and joined planes of the (111) type. The image contrast obtained in the simulation resembles the contrast displayed in the experimental HREM images.

particle obtained from the 0.044 mmol/50 ml gold ion concentration. The theoretical simulation was obtained assuming a model of two fcc crystals along the [011] orientation and joined on (111) lattice planes. The image contrast displayed in Fig. 8c resembles the digitized HREM image contrast of Fig. 8b.

To understand the effects of the energy in the formation of a specific configuration, we performed a geometrical optimization of the clusters. In Table 1, the binding energies for the different calculated models are shown, basically with examples of cubo-octahedral configurations with 13, 19 and 38 atoms and decahedral

Table 1
Binding and frontier molecular orbital energy and the corresponding gap for different configurations

Structure	Number of Au atoms	Binding energy per atom (eV)	HOMO (eV)	LUMO (eV)	Gap (eV)
Cubo-octahedral	13	−1.376	−3.715	−3.061	−0.654
	19	−1.506	−3.650	−3.172	−0.479
	38	−1.156	−3.791	−3.118	−0.673
Decahedral	13	−1.349	−3.460	−3.196	−0.264
	19	−1.448	−3.414	−3.062	−0.352
	39	−1.163	−3.252	−2.790	−0.461

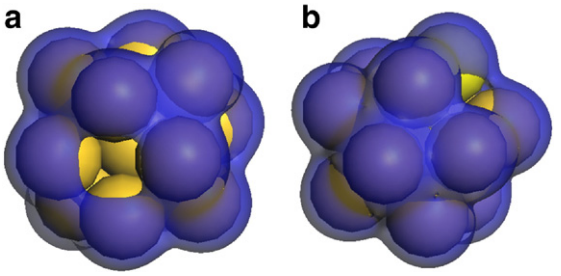

Fig. 9. Electrophilic fields determined by the Fukui functions calculations 0.0025 eV iso-value distribution for the structure: a) cubo-octahedral Au_{13} and b) decahedral Au_{13}.

configurations with 13, 19 and 39 atoms, besides the energy gap between HOMO and LUMO for each of the models. From the binding energy values, it is clear that the lowest energy is the Au_{13} fcc-like configuration. In addition, the binding energies of the different configurations with the same number of atoms varied slightly; however in general the trend to cubic-like structures with a lower energy was observed. It has been reported in the past [17] that the binding energy of small particles is dependent on the number of atoms, while the structure/configuration has no influence. From the energy gap values, we can observe that the decahedral structure Au_{13} have the lowest energy HOMO–LUMO gap, which is due to the higher density of electrons on its surface. Therefore, we can say that in the case of Au, the decahedral structures are favorable when the particle size is small, and when the particle size increases, the cubo-octahedral structures become more favorable. In Fig. 9, the electrophilic fields determined by Fukui functions for both cubo-octahedral and decahedral structures are presented. For both the structures, the 0.0025 eV iso-value distributions are displayed. It is clear that the electrophilic field of the cubo-octahedron configuration is localized on the vortices, and for the decahedron configuration, the electrophilic field is localized on the face with five-fold symmetry. Thus, small decahedral structures exhibit superior catalytic activity than cubo-octahedral structures.

4. Conclusions

Gold nanoparticles with narrow size distributions have been prepared using a chemical reduction method. The size of gold nanoparticles increases as the concentration of gold ions in the reaction mixture increases. For a lower concentration of the metal ions, the commonly found structures are decahedral and fcc-deformed. However, when the concentration is increased, the structure changes to single twinned and fcc. The theoretical analysis by a quantum mechanical approach reveals that the electronic structure of nanoparticles is significantly affected by their atomic configurations; inducing higher catalytic activity for decahedral configurations when five-fold faces are exposed. However, due to the coexistence of structures such as fcc-like and decahedral in the synthesized sample, the material must have a highly dispersed activation energy suitable for wide range of catalytic applications.

Acknowledgments

We would like to acknowledge the technical support of A. Medina for the high-resolution electron microscopy. The work is partially supported by VIEP-BUAP (Grant No. 11/I/EXC/05).

References

[1] Takasu YY, Kawaguchi T, Sugimoto W, Murakami Y. Effects of the surface area of carbon support on the characteristics of highly-dispersed Pt–Ru particles as catalysts for methanol oxidation. Electrochim Acta 2003;48:3861–8.
[2] Roth C, Goetz M, Fuess H. Synthesis and characterization of carbon-supported Pt–Ru–WO*x* catalysts by spectroscopic and diffraction methods. J Appl Electrochem 2001;31:793–8.
[3] Zaluska A, Zaluski L, Ström-Olsen JO. Structure, catalysis and atomic reactions on the nano-scale: a systematic approach to metal hydrides for hydrogen storage. Appl Phys 2001; A72:157–65.
[4] Bell AT. The impact of nanoscience on heterogeneous catalysis. Science 2003;299:1688–91.
[5] Ascencio JA, Gutiérrez-Wing C, Espinosa-Pesqueira ME, Marín M, Tehuacanero S, Zorrilla C, et al. Structure determination of small particles by HREM imaging: theory and experiment. Surf Sci 1998;396:349–68.
[6] Esparza R, Ascencio JA, Rosas G, Sánchez JF, Pal U, Pérez R. Structure, stability and catalytic activity of chemically synthesized Pt, Au, and Au–Pt nanoparticles. J Nanosci Nanotech 2005;5:641–7.
[7] Pal U, Sanchez JF, Gamboa SA, Sebastian PJ, Pérez R. Drastic improvement of properties of Nafion 112 by impregnation of Au/Pd nanoclusters. Phys Stat Solid 2003;C8:2944–8.
[8] Gómez A, Beltrán del Río LM. SimulaTEM. Rev Latinoam Metal Mater 2001;21:46–50.
[9] Delley B. From molecules to solids with the $DMol^3$ approach. J Chem Phys 2000;113:7756–64.
[10] Perdew JP, Wang Y. Accurate and simple analytic representation of the electron-gas correlation energy. Phys Rev 1992; B45:13244–9.
[11] Rodriguez-Lopez JL, Montejano-Carrizales JM, Pal U, Sanchez-Ramirez JF, Troiani HE, Garcia D, et al. Surface reconstruction and decahedral structure of bimetallic nanoparticles. Phys Rev Lett 2004;92:196102–5.
[12] Liu HB, Pal U, Pérez R, Ascencio JA. Structural transformation of Au–Pd bimetallic nanoclusters on thermal heating and cooling: a dynamic analysis. J Phys Chem 2006;B110:5191–5.
[13] Ascencio JA, Gutiérrez-Wing C, Espinosa-Pesqueira ME, Marín M, Tehuacanero S, Zorrilla C, et al. Structure determination of

small particles by HREM imaging: theory and experiment. Surf Sci 1998;396:349–69.
[14] Liu HB, Pal U, Medina A, Maldonado C, Ascencio JA. Structural incoherency and structure reversal in bimetallic Au–Pd nanoclusters. Phys Rev 2005;B71:075403.
[15] Erkoç S. Stability of gold clusters: molecular-dynamics simulations. Phys E: Low-Dim Syst Nanos 2000;8:210–8.
[16] Garzón IL, Michaelian K, Beltrán MR, Posada-Amarillas A, Ordejon P, Artacho E, et al. Structure and thermal stability of gold nanoclusters: the Au-38 case. Eur Phys J 1999;D9:211–5.
[17] Cleveland CL, Landman U, Schaaff TG, Shafigullin MN, Stephens PW, Whetten RL. Structural evolution of smaller gold nanocrystals: the truncated decahedral motif. Phys Rev Lett 1997;79:1873–6.